Anisotropic Excitation Spectrum of a Dipolar Quantum Bose Gas

G. Bismut, B. Laburthe-Tolra, E. Maréchal, P. Pedri, O. Gorceix, and L. Vernac

Laboratoire de Physique des Lasers, UMR 7538 CNRS, Université Paris 13, 99 Avenue J.-B. Clément, 93430 Villetaneuse, France

(Received 25 May 2012; published 9 October 2012)

We measure the excitation spectrum of a dipolar chromium Bose-Einstein condensate with Raman-Bragg spectroscopy. The energy spectrum depends on the orientation of the dipoles with respect to the excitation momentum, demonstrating an anisotropy that originates from the dipole-dipole interactions between the atoms. We compare our results with the Bogoliubov theory based on the local density approximation and, at large excitation wavelengths, with the numerical simulations of the time-dependent Gross-Pitaevskii equation. Our results show an anisotropy of the speed of sound.

DOI: 10.1103/PhysRevLett.109.155302 PACS numbers: 67.85.De, 32.80.Qk, 37.10.Vz, 47.37.+q

Interactions play a major role in the physics of Bose-Einstein condensates (BECs), made of trapped neutral atoms. Attractive interactions may lead to a collapse [1], while repulsive interactions confer a collective nature to excitations [2] and lead to superfluidity [3]. In the first produced BECs, only contact interactions played a significant role. The study of long-range anisotropic (partially attractive) dipole-dipole interactions (DDIs) in quantum gases was initiated by the production of chromium BECs [4], followed more recently by experiments with dysprosium [5,6] and erbium [7]. DDIs introduce anisotropy in the expansion dynamics [8] and the collective excitations of a Cr BEC [9]. Moreover, when DDIs overwhelm the contact interactions, a BEC undergoes a characteristic d-wave-like implosion, revealing the structure of the DDIs [7,10]. While these already observed dipolar effects are sensitive to trap geometry, DDIs can also modify the bulk properties of quantum gases, independent of geometry. In particular, DDIs may lead to anisotropic superfluidity in Bose [11] or Fermi gases [12], with possible analogies to anisotropic superconductivity in cuprates. In this Letter, we study the elementary excitations of a Cr BEC and show an anisotropic excitation spectrum, providing a signature of an anisotropy of the speed of sound and, therefore, according to the Landau criterion, a possibility for anisotropic superfluidity.

Raman-Bragg spectroscopy, creating elementary excitations with a well-defined momentum, has developed into a powerful instrument to study the bulk properties of quantum gases [13]. Following the first seminal demonstration that rapidly followed the creation of atomic BECs [14,15], a more systematic series of experiments gave a full picture of the BEC excitation spectrum from the low-energy phonon-like excitations to the high-energy single-particle regime [16]. Despite several reviews and theoretical papers pointing out the interest in the excitation spectrum of bosonic gases featuring DDIs [17–19], experimental results are not yet available. See, however, the recent works on effective long-range interactions in optical lattices [20]. Chromium atoms away from a Feshbach resonance are particularly suitable to study the bulk properties of dipolar BECs, since DDIs are non-negligible, without leading to collapse. In this Letter, we provide the first evidence that long-range dipolar interactions induce an anisotropy of a BEC excitation spectrum using Raman-Bragg spectroscopy. The spectrum is anisotropic as the resonance condition depends on the angle θ between the polarization axis parallel to the magnetic field $\mathbf{B}$ and the excitation wave vector $\mathbf{q}$ (see Fig. 1). We probe this anisotropy throughout the whole excitation spectrum with differential

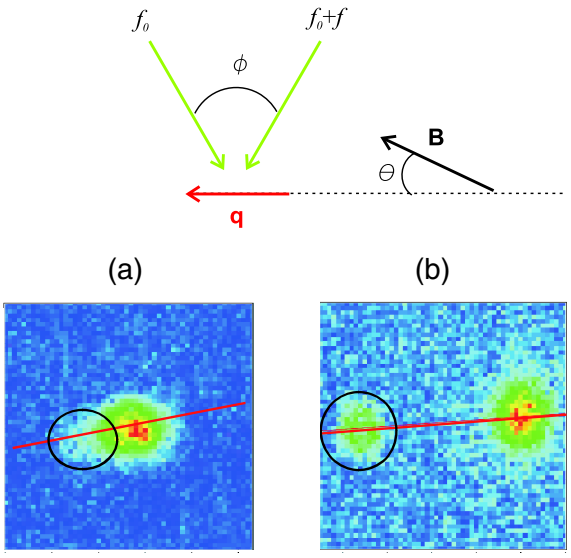

FIG. 1 (color online). The principle of the experiment and absorption pictures after a Bragg pulse. The two Bragg beams are coupled to the BEC with an angle ϕ, and transfer a momentum $\hbar_{\mathbf{q}}$ and an energy hf to the excited fraction. Because of DDIs, the excitation spectrum depends on the angle θ between $\mathbf{q}$ and $\mathbf{B}$. The two absorption pictures, in false color, show the density after Bragg pulse and time of flight, and the solid lines indicate the direction of momentum transfer. In (a), the small value of ϕ (14°), and hence of q, barely allows spatial separation of the excited fraction, contrary to the case of large ϕ (82°) in (b).

measurements for two orthogonal orientations of the magnetic field, either parallel or orthogonal to $\mathbf{q}$.

The anisotropy of the excitation spectrum for an homogenous dipolar BEC is well understood within the Bogoliubov theory [17]:

$$\epsilon(\mathbf{q}) = \left[\frac{\hbar^2 q^2}{2m}\left(\frac{\hbar^2 q^2}{2m} + 2gn[1 + \epsilon_{dd}(3\cos^2\theta - 1)]\right)\right]^{1/2}, \quad (1)$$

where $\epsilon(\mathbf{q})$ and $\mathbf{q}$ are, respectively, the energy and wave vector of the excitation, m the atom mass, n the atomic density, and $g = 4\pi\hbar^2 a/m$ (with a the scattering length); ϵ_{dd} is the dimensionless parameter scaling the relative importance of dipolar interactions with respect to contact interactions. For magnetic DDIs, $\epsilon_{dd} = \mu_0\mu_m^2 m/12\pi\hbar^2 a$ (μ_0 is the vacuum permeability, μ_m the atom magnetic moment equal to six Bohr magnetons for Cr). In the absence of DDIs ($\epsilon_{dd} = 0$), one recovers the known spectrum for a BEC with only contact interactions [21]. For Cr, ϵ_{dd} is 0.16 (with $a = 102.5a_0$ [22]), which allows us to explore the anisotropic character of Eq. (1) more easily than for alkali BECs (e.g., $\epsilon_{dd} = 0.01$ for Rb). The angular dependance of Eq. (1), related to the fact that the Fourier transform of DDIs depends on the relative momentum of the particles (contrarily to the case of delta potential interactions), can be interpreted as an attractive contribution (repulsive) of DDIs to the excitation energy for the perpendicular (parallel) case [17].

According to Eq. (1), the sound velocity defined as $c_\theta = \lim_{q\to 0}\frac{\epsilon(\mathbf{q})}{q}$ becomes anisotropic. It is maximal in the parallel ($\theta = 0$) geometry, while it is minimal in the perpendicular ($\theta = \pi/2$) geometry. Defining the velocity without DDIs $c_0 = (gn/m)^{1/2}$, one obtains $c_\parallel = c_0(1 + 2\epsilon_{dd})^{1/2}$ and $c_\perp = c_0(1 - \epsilon_{dd})^{1/2}$, so that $c_\parallel/c_\perp = 1.25$ for Cr. This relative dipolar shift of 25% is larger than in previous experiments with Cr BECs [8,9], where shifts remained in a lower percentage range (much less than ϵ_{dd}), as a result of angular averaging of DDIs in the BEC [8,23]. The situation is quite different for the bulk BEC excitations described by Eq. (1), as there is no such angular averaging: θ has the same value for all the atoms.

To obtain the experimental excitation spectra, we first create a chromium BEC in a crossed-beam dipole trap. Details on the experimental setup and the procedures can be found in Ref. [24]. The BEC, comprising about 10 000 atoms polarized in the absolute ground (Zeeman) state, is confined at the bottom of the trap with frequencies $(\omega_x, \omega_y, \omega_z) = 2\pi \times (145, 180, 260)$ Hz, within a magnetic field of $B = 50$ m Gauss. To impart a momentum q to a fraction of the condensed atoms, we use two intersecting phase-locked focused laser beams derived from the same single-mode solid-state laser ($\lambda = 532$ nm). Two acousto-optic modulators shift the beam frequencies by, respectively, Ω and $\Omega + 2\pi f$, with $\Omega = 2\pi \times 80$ MHz. At the atom location, the respective waists of the laser beams are 40 and 32 μm, while their powers are between 500 and 1000 μW. The beam intensities are chosen to limit the excited fraction to about 15% which ensures a good trade-off between the validity of the perturbative Bogoliubov approach for theoretical interpretation and the signal-to-noise ratio. The angle ϕ between the beams propagating directions sets the momentum value $q[q = 2\pi/\lambda \times \sin(\phi/2)]$, while the energy difference hf, equal to the energy of the excitation, is adjustable at will. Although the optical access restricts the accessible values for ϕ, thus also those for q, we have been able to probe the dispersion relation from the phonon to the free-particle regime.

The two beams, hereafter referred to as the Raman beams, are switched on only for a brief pulse time. Raman transitions are efficiently driven between the rest ground state and the excited states, with momentum q and energy hf, when the beam photon energy difference matches the excitation energy, i.e., when the Raman-Stokes resonance condition is met. Since the process can be interpreted as diffraction of the matter wave onto the moving lattice created by the Raman beams, the whole process is often referred to as Bragg spectroscopy of the excitation spectrum of the BEC. To ensure that the momentum of the atoms is solely set by the Bragg pulse (and is not modified by trap dynamics), the pulse duration τ_{Bragg} should be far less than the oscillation periods in the trap [14]. Meeting this requirement causes a strong Fourier broadening, and we found a trade-off by setting $\tau_{\text{Bragg}} = 1.5$ ms: the Fourier broadening (half width at $1/e^2 = 300$ Hz) is then smaller that the experimental spectra widths, and spatial separations between the excited fraction and the ground state are close to the ones expected from the Bragg momentum transfer ($\hbar q/m \times$ expansion time; see below).

We measure the atom momentum distribution by releasing the atoms from the trap after the Bragg pulse and by performing absorption imaging after an expansion time of 5 ms (see Fig. 1). From the density profiles of these distributions along the excitation direction [25], we infer the excited fraction $P_{\text{exc}} = [N_{\text{exc}}/(N_{\text{exc}} + N_0)]$, where N_{exc} is the number of excited atoms and N_0 the number of atoms remaining in the ground $q \sim 0$ state. We record the Bragg spectra by monitoring the excited fraction versus f for a given value of ϕ. It is clear from Fig. 2 that the excitation energy spectrum for parallel polarization is shifted towards high frequency with respect to the spectrum for orthogonal polarization, as expected from Eq. (1).

The results of Eq. (1) hold only in the homogeneous case. With trapped gases, two kinds of finite size effects have to be taken into account, which are sources of spectral broadenings: the density inhomogeneity in the trap, and the nonzero width-momentum distribution (inducing Doppler effect), which are dominant, respectively, at low and high

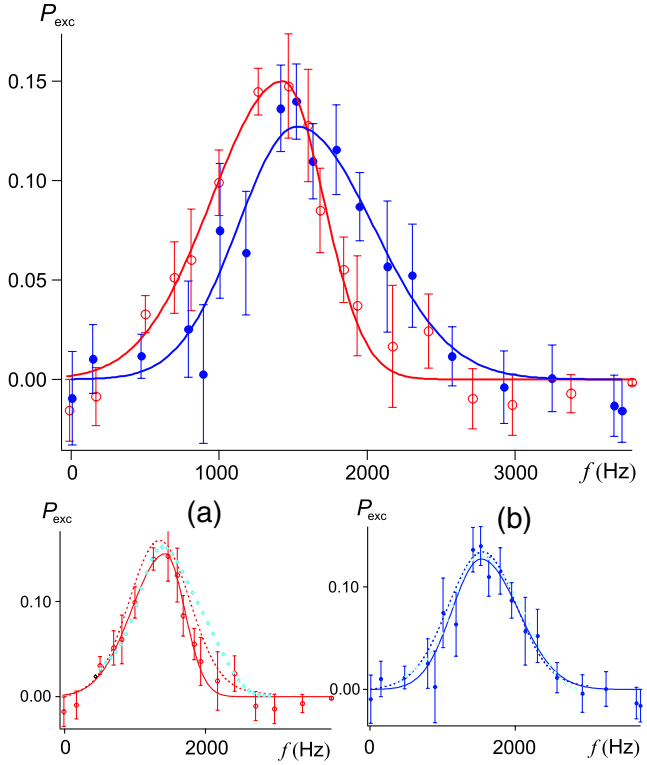

FIG. 2 (color online). Excitation spectra for $q\xi_0 = 0.8$ ($\phi = 14$ deg). The excited fraction P_{exc} is plotted versus the detuning frequency f between the two Bragg beams for $\theta = 0$ (filled circles) and $\theta = \pi/2$ (open circles). The two solid lines are asymmetric Gaussian fits to the data (see text). The error bars represent the 1-sigma statistical uncertainty associated to three measurements. The two spectra are shown separately below (a) $\theta = \pi/2$, (b) $\theta = 0$ along with the results of our linear response theory (dashed lines), which has no adjustable parameters, and of our numerical simulations (diamonds).

excitation momentum [26]. To account for our experimental results, we extended the theory developed in Ref. [26] based on local density approximation (LDA) by including DDIs. The validity of LDA with DDIs, discussed in Ref. [18], is guaranteed if $q \gg 1/R_{\mathrm{TF\,min}}$ [27], with $R_{\mathrm{TF\,min}}$ the smallest BEC Thomas-Fermi (TF) radius. Then, the BEC can be considered as a locally homogeneous 3D system [28]; $q \gg 1/R_{\mathrm{TF\,min}}$ also ensures that the effects of energy discretization can be safely neglected.

For a comparison with our experimental spectra (see Fig. 2), we take into account the Doppler width and make a convolution between the corresponding Gaussian and the LDA excitation spectrum [29]. The Fourier broadening due to the finite excitation duration is also taken into account within the linear response theory [30]. The two-photon Raman frequency Ω_R, which sets the excitation amplitude [16], is estimated from a calibration of the lattice depth created by the Raman beams [31]. The agreement with theory (with no adjustable parameter) of the spectra line shapes is good, except for the two lowest experimental values of q. For the excitation amplitude, the discrepancy remains at most in the 50% range for all spectra. All features are in very good agreement in the case of Fig. 2, for which we estimate $\Omega_R = 2\pi \times (140 \pm 30)$ Hz.

We have performed a study of the effects of DDIs by probing the excitation spectrum as a function of q from the phonon regime to the free-particle regime (see Fig. 3). We define the experimental value of $\epsilon(\mathbf{q})$ as the mean value of the excitation energy, obtained by using asymmetric Gaussian fits of the excitation spectra; this procedure empirically takes into account the nonsymmetric nature of the excitation spectra, which is expected from the Thomas-Fermi distribution (see for example Ref. [26]). We define $\epsilon_{\parallel}(q)$ [respectively, $\epsilon_{\perp}(q)$] as the mean value obtained for

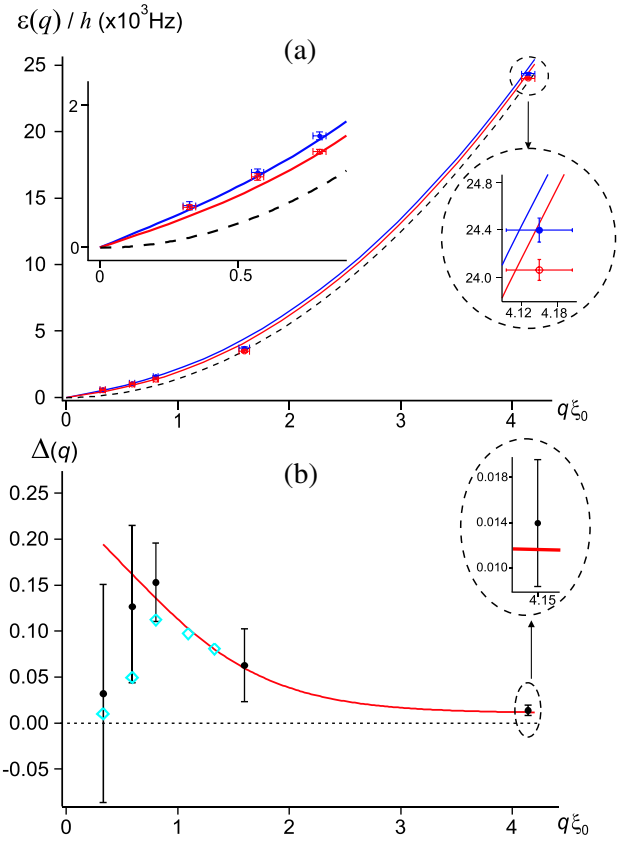

FIG. 3 (color online). (a) Energy spectra: the energy $\epsilon(\mathbf{q})$ divided by h is plotted as a function of Bragg-transferred momentum q. The circles correspond to the experimental data: for a given value of q, the top (bottom) circle corresponds to the parallel (perpendicular) case. The point at $q\xi_0 = 1.6$ corresponds to a four-photon process (see text). The two solid lines are the results of LDA calculations for parallel (top line) and orthogonal (bottom line) cases. The dashed line gives the results for a free particle. Inset: zoom for low q values. (b) Relative shift $\Delta(q)$ of the excitation energies (see text) as a function of q. Black points: results of fits of the experimental data, with error bars. Solid line: results of LDA calculations. The diamonds show the results of numerical simulations. For (a) and (b), the vertical error bars represent 1σ statistical uncertainty, while the horizontal ones correspond to uncertainties on the values of ϕ.

the parallel (orthogonal) case. Figure 3(a) shows the corresponding data. We use the DDI-independent healing length $\xi_0 = \hbar/(2mgn_0)^{1/2}$ (with n_0 the measured BEC peak density) to normalize the q axis: ξ_0 indicates the frontier between the phonon domain ($q\xi_0 < 1$) and the single-particle domain ($q\xi_0 \gg 1$). The data correspond to four ϕ angles. To fill the gap between the accessible low (6°, 10°, and 14°) and the high (82°) values of ϕ, we realized a four-photon Raman-like excitation [32] to obtain data for another q value [$q = 4\pi/\lambda \times \sin(14°/2)$, and $q\xi_0 = 1.6$]. The horizontal error bars are mainly set by the uncertainty on the experimental value of ϕ, and the vertical ones are determined by applying a bootstrapping procedure [33] to the experimental data. We compare the predictions of our theory assuming a constant (10^4) number of atoms with the corresponding experimental data in Fig. 3(a) [34]. We obtain a good general agreement between the data and theory with no free parameter; some of the discrepancies may originate from an underestimation of the uncertainties on the values of ϕ.

To emphasize how the two dispersion curves differ, we plot in Fig. 3(b) the relative variation of $\epsilon(\mathbf{q})$, $\Delta(q) = 2\frac{\epsilon_\parallel(q)-\epsilon_\perp(q)}{\epsilon_\parallel(q)+\epsilon_\perp(q)}$. We measure an anisotropy of the excitation spectrum of the Cr BEC, both in the low q limit and the high q limit. As the systematic effects on $\Delta(q)$ related to changes in trapping frequencies and atom number induced by the change in θ remain negligible (from at most 1.5% at low q to below 0.1% at high q), our results demonstrate a DDI-induced anisotropy of the excitation spectrum. The agreement with our linear response theory is relatively good, except for the lowest value of q. This is not surprising, since then the excitation wavelength is larger than the BEC Thomas-Fermi diameter (equal to 7 μm). For long wavelengths, discrete modes can be excited, for which the effects of DDIs are much smaller than for phonons, as observed in Ref. [9]. We have therefore solved numerically the time-dependent 3D Gross-Pitaevskii equation including contact interactions and DDIs. Our numerical simulations are in rather good agreement with our experimental data [see Fig. 3(b)], and show that relative shifts significantly smaller than the ones obtained with the LDA theory are expected as the excitation wavelength increases.

We finally rely on the LDA theory to extract quantitative values for the sound velocity from our experimental data. In our case, the extensive experimental study of the linear phonon part of the spectrum is not accessible owing to the small size of our BEC (in contrast to Ref. [16]). We therefore chose to derive sound velocities from the data at $q\xi_0 = 0.8$, as this is the lowest value of q for which we find a good agreement with the LDA theory. The corresponding excitation frequency (around 1.5 kHz) is significantly higher than the trap frequencies, which explains why the energy discretization effects are small. From the experimental values $\epsilon_\parallel/h = (1.57 \pm 0.05)$ kHz and $\epsilon_\perp/h = (1.35 \pm 0.03)$ kHz, we derive sound velocities through the linear response theory. The Feynman law (see Ref. [16]) relates the average energy $\epsilon_\mathbf{q}$ to the (LDA averaged) static structure factor $S_\mathbf{q}$: $\epsilon_\mathbf{q} = \frac{\epsilon^0_\mathbf{q}}{S_\mathbf{q}}$, with $\epsilon^0_\mathbf{q} = \hbar^2q^2/2m$ the free-particle energy, and $S_\mathbf{q}$ is related to c_θ through $S_\mathbf{q} = \frac{15}{4}\left\{\frac{3+\alpha_\mathbf{q}}{4\alpha_\mathbf{q}^2} - \frac{(3+2\alpha_\mathbf{q}-\alpha_\mathbf{q}^2)}{16\alpha_\mathbf{q}^{5/2}}\left[\pi + 2\arctan\left(\frac{\alpha_\mathbf{q}-1}{2\sqrt{\alpha_\mathbf{q}}}\right)\right]\right\}$, where $\alpha_\mathbf{q} = 2m(15\pi c_\theta/32)^2/\epsilon^0_\mathbf{q}$. We obtain $c_\perp = 2.06 \pm 0.05\ \mathrm{mm\cdot s^{-1}}$ and $c_\parallel = 2.64 \pm 0.1\ \mathrm{mm\cdot s^{-1}}$, in good agreement with the LDA predictions in our experimental conditions equal to $2.02 \pm 0.05\ \mathrm{mm\cdot s^{-1}}$ and $2.53 \pm 0.05\ \mathrm{mm\cdot s^{-1}}$, respectively, $-c_{\theta,\mathrm{LDA}} = \frac{32}{15\pi}\left\{\frac{gn_0}{m}[1 + \epsilon_{dd}(3\cos^2\theta - 1)]\right\}^{1/2}$.

In this Letter, we have shown that the excitation spectrum of a spin-polarized chromium BEC is anisotropic as a consequence of the dipolar character of the interactions between the atoms. As long as the wave vector is not too small compared to the inverse of the BEC size, our experimental results are correctly accounted for by a linear response theory based on the Bogoliubov approach. The demonstrated existence of an anisotropic speed of sound raises the question of anisotropic superfluidity, for example, how excitations in different directions couple. Extension of our work to BECs with larger DDIs could allow the discovery of rotonic features in the excitation spectrum [35] of quasi-2D BECs.

LPL is Unité Mixte (UMR 7538) of CNRS and of Université Paris 13. We acknowledge financial support from Conseil Régional d'Ile-de-France (CPER), Ministère de l'Enseignement Supérieur et de la Recherche, and IFRAF.

[1] R. J. Dodd, M. Edwards, C. J. Williams, C. W. Clark, M. J. Holland, P. A. Ruprecht, and K. Burnett, Phys. Rev. A **54**, 661 (1996).
[2] M.-O. Mewes, M. R. Andrews, N. J. van Druten, D. M. Kurn, D. S. Durfee, C. G. Townsend, and W. Ketterle, Phys. Rev. Lett. **77**, 988 (1996).
[3] R. Onofrio, C. Raman, J. M. Vogels, J. R. Abo-Shaeer, A. P. Chikkatur, and W. Ketterle, Phys. Rev. Lett. **85**, 2228 (2000).
[4] A. Griesmaier, J. Werner, S. Hensler, J. Stuhler, and T. Pfau, Phys. Rev. Lett. **94**, 160 401 (2005).
[5] M. Lu, N. Q. Burdick, S. H. Youn, and B. L. Lev, Phys. Rev. Lett. **107**, 190 401 (2011).
[6] M. Lu, N. Q. Burdick, and B. L. Lev, Phys. Rev. Lett. **108**, 215 301 (2012).
[7] K. Aikawa, A. Frisch, M. Mark, S. Baier, A. Rietzler, R. Grimm, and F. Ferlaino, Phys. Rev. Lett. **108**, 210 401 (2012).
[8] J. Stuhler, A. Griesmaier, T. Koch, M. Fattori, T. Pfau, S. Giovanazzi, P. Pedri, and L. Santos, Phys. Rev. Lett. **95**, 150 406 (2005).
[9] G. Bismut, B. Pasquiou, E. Maréchal, P. Pedri, L. Vernac, O. Gorceix, and B. Laburthe-Tolra, Phys. Rev. Lett. **105**, 040404 (2010).

[10] T. Lahaye, J. Metz, B. Fröhlich, T. Koch, M. Meister, A. Griesmaier, T. Pfau, H. Saito, Y. Kawaguchi, and M. Ueda, Phys. Rev. Lett. **101**, 080401 (2008).
[11] C. Ticknor, R. M. Wilson, and J. L. Bohn, Phys. Rev. Lett. **106**, 065301 (2011).
[12] M. A. Baranov, M. S. Marenko, V. S. Rychkov, and G. V. Shlyapnikov, Phys. Rev. A **66**, 013606 (2002).
[13] R. Ozeri, N. Katz, J. Steinhauer, and N. Davidson, Rev. Mod. Phys. **77**, 187 (2005).
[14] J. Stenger, S. Inouye, A. P. Chikkatur, D. M. Stamper-Kurn, D. E. Pritchard, and W. Ketterle, Phys. Rev. Lett. **82**, 4569 (1999).
[15] D. M. Stamper-Kurn, A. P. Chikkatur, A. Görlitz, S. Inouye, S. Gupta, D. E. Pritchard, and W. Ketterle, Phys. Rev. Lett. **83**, 2876 (1999).
[16] J. Steinhauer, R. Ozeri, N. Katz, and N. Davidson, Phys. Rev. Lett. **88**, 120 407 (2002).
[17] T. Lahaye, C. Menotti, L. Santos, M. Lewenstein, and T. Pfau, Rep. Prog. Phys. **72**, 126401 (2009).
[18] A. R. P. Lima and A. Pelster, arXiv:1111.0900.
[19] P. Muruganandam and S. K. Adhikari, Phys. Lett. A **376**, 480 (2012)
[20] R. Mottl, F. Brennecke, K. Baumann, R. Landig, T. Donner, and T. Esslinger, Science **336**, 1570 (2012).
[21] L. Pitaevskii and S. Stringari, *Bose-Einstein Condensation* (Oxford Science Publications, Oxford, 2003).
[22] B. Pasquiou, G. Bismut, Q. Beaufils, A. Crubellier, E. Maréchal, P. Pedri, L. Vernac, O. Gorceix, and B. Laburthe-Tolra, Phys. Rev. A **81**, 042716 (2010).
[23] S. Giovanazzi, L. Santos, and T. Pfau, Phys. Rev. A **75**, 015604 (2007).
[24] Q. Beaufils, R. Chicireanu, T. Zanon, B. Laburthe-Tolra, E. Maréchal, L. Vernac, J.-C. Keller, and O. Gorceix, Phys. Rev. A **77**, 061601 (2008); G. Bismut, B. Pasquiou, D. Ciampini, B. Laburthe-Tolra, E. Maréchal, L. Vernac, and O. Gorceix, Appl. Phys. B **102**, 1 (2011).
[25] At small q, we also evaluate the excited fraction by measuring the total momentum transferred to the cloud, as in Ref. [16]; the two methods give very similar results.
[26] F. Zambelli, L. Pitaevskii, D. M. Stamper-Kurn, and S. Stringari, Phys. Rev. A **61**, 063608 (2000).
[27] G. Bismut, Ph.D. thesis, Université Paris 13, March 2012.
[28] In lower dimensions systems, the effects of DDIs on the Bogoliubov excitation energy are totally different than in the 3D case (see Ref. [19]).
[29] D. Stamper-Kurn and W. Ketterle, in *Les Houches, Session LXXII, Coherent Atomic Matter Waves*, edited by R. Kaiser, C. Westbrook, and F. David (Springer-Verlag, Berlin, 2001).
[30] A. Brunello, F. Dalfovo, L. Pitaevskii, S. Stringari, and F. Zambelli, Phys. Rev. A **64**, 063614 (2001).
[31] At low q, for which diffraction orders overlap, the calibration is set by the maximum momentum imparted to the BEC by long pulses [see J. H. Huckans, I. B. Spielman, B. L. Tolra, W. D. Phillips, and J. V. Porto, Phys. Rev. A **80**, 043609 (2009)].
[32] M. Kozuma, L. Deng, E. W. Hagley, J. Wen, R. Lutwak, K. Helmerson, S. L. Rolston, and W. D. Phillips, Phys. Rev. Lett. **82**, 871 (1999).
[33] B. Efron, Ann. Stat. **7**, 1 (1979).
[34] As proven in Ref. [26], Doppler broadening does not change the average excitation energy predicted by LDA, so that the calculations in Fig. 3 are also in fact LDA results.
[35] D. H. J. O'Dell, S. Giovanazzi, and G. Kurizki, Phys. Rev. Lett. **90**, 110 402 (2003); L. Santos, G. V. Shlyapnikov, and M. Lewenstein, Phys. Rev. Lett. **90**, 250 403 (2003).